Development of a topology-based current-flux characteristic approximation in a Hamiltonian model of a reluctance machine[*]

WOJCIECH BURLIKOWSKI, ZYGMUNT KOWALIK

Silesian University of Technology
Faculty of Electrical Engineering
Department of Mechatronics
ul. Akademicka 10a, 44-100, Gliwice, Poland
e-mail: {wojciech.burlikowski/zygmunt.kowalik}@polsl.pl

Abstract: The paper presents an algorithm for the construction of an approximation of a highly nonlinear current-flux characteristic of a synchronous reluctance machine. Such an approximation is required in a Hamiltonian model of an electric machine and the constructed approximation is suited to be used in such a model. It employs a simplicial approximation based on irregular points sets in the spaces of currents and fluxes. The sets are constructed by the iterative insertion of new points. Initially the sets contain an arbitrarily small number of elements. The insertion is based on an approximation error calculation. Based on the sets containing possibly small number of elements, the proposed procedure leads to smooth and precise approximation. Due to the nonlinearity of the approximated characteristics, ambiguities can occur. A method for the triangulation refinement of the sets of currents and fluxes that eliminates them is also presented. In the paper, a reluctance machine model using the constructed approximation is described and compared with a model using the approximation based on regular sets.

Key words: Hamiltonian model, simplicial approximation, reluctance machine, triangulation refinement

1. Introduction

A Hamiltonian model of a reluctance machine requires an approximation of its current-flux characteristics. Such an approximation can be made using a simplicial approximation, which for a given set of flux linkages (phase or line-to-line) and a corresponding set of phase currents, approximates linearly a needed characteristic in each simplex of triangulated sets of vertices (points) in both the space of currents and fluxes. The mathematical description of simplicial approximation is given in [1].

---

[*] This is extended version of paper which was presented at the 23th Symposium on Electromagnetic Phenomena in Nonlinear Circuits, Pilsen, Czech Republic 02-04.07.2014.

In this paper, an algorithm used for the construction of points sets, that the simplicial approximation is based on, is shown. The algorithm is based on approximation error calculations and an insertion of the new points into the sets to make the approximation more precise in very nonlinear areas of the approximated current-flux characteristic. The presented algorithm is then used to construct the approximation of a current-flux characteristic of a synchronous reluctance machine (SynRM), as in this machine nonlinear effects caused by magnetic saturation are very significant. The constructed approximation is used in a Hamiltonian model of this SynRM machine and the performance of the model is analyzed.

2. The considered Hamiltonian model of a SynRM machine

In this paper a model of a 3-phase SynRM machine with a wye connected stator winding without a neutral wire is considered. Such a model is described in [2], and a scheme of this model is shown in Figure 1. Such a connection scheme is considered due to its great practical importance. It also reduces the number of state variables describing an electromechanical system, which strongly simplifies the approximation error computation and the approximation refinement.
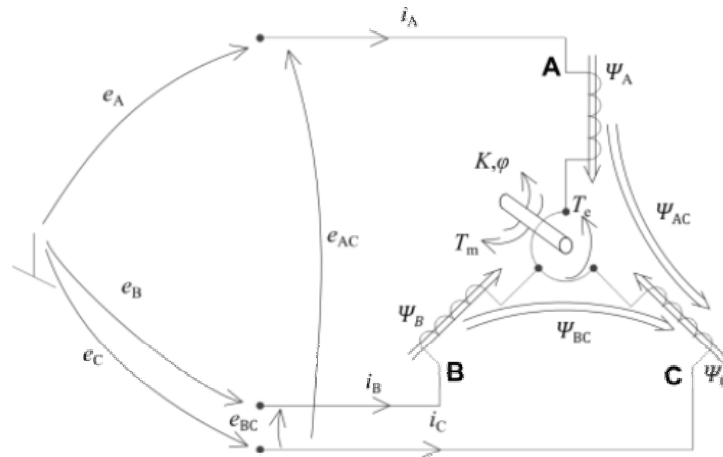

Fig. 1. A scheme of a considered SynRM machine model

An equation describing an electrical part of this model is given by (1).

$$\frac{d}{dt}\Psi = \boldsymbol{e} - \begin{bmatrix} r_A + r_C & r_C \\ r_C & r_B + r_C \end{bmatrix} \boldsymbol{i}(\Psi, \varphi),$$

(1)

where: r_A, r_B, r_C – respective phase resistances, φ – rotor angular position, $\boldsymbol{e} = [e_{AC}; e_{BC}]^{\mathrm{T}}$ – line-to-line voltages vector, $\boldsymbol{\Psi} = [\Psi_{AC}; \Psi_{BC}]^{\mathrm{T}}$ – line-to-line flux linkages vector, whose components are $\Psi_{AC} = \Psi_A - \Psi_C$, $\Psi_{AB} = \Psi_B - \Psi_C$, $\boldsymbol{i}(\boldsymbol{\Psi}, \varphi) = [i_A(\boldsymbol{\Psi}, \varphi); i_B(\boldsymbol{\Psi}, \varphi)]$ – phase currents vector, being a function of flux linkages and rotor angular position.

With a fixed rotor angular position $\varphi = const$, a function $h: \boldsymbol{\Psi} \to \boldsymbol{i}$ transforms an area in the space of fluxes $\boldsymbol{R\Psi} \in \mathbb{R}^2$ onto an area in the space of currents $\boldsymbol{RI} \in \mathbb{R}^2$. Function $\boldsymbol{i} = h(\boldsymbol{\Psi})$ is a homeomorphism, so the construction of vertices sets in both spaces can be made considering the inverse function $h^{-1}: \boldsymbol{\Psi} \to \boldsymbol{i}$. This fact enables the usage of the finite elements method (FEM) for the construction of these points sets, as in the FEM currents are typically independent variables.

3. Construction of currents and fluxes sets for a simplicial approximation

Figure 2 shows a surface representation of one component of a h^{-1} function, that is a $\Psi_{AC} = g(i_A, i_B)$ function, obtained using FEM for the exemplary SynRM machine – the shown representation is actually a piecewise linear approximation of the $\Psi_{AC}(i_A, i_B)$ function, nodes of which are obtained by magnetostatic FEM computation. This, and all further FEM computation were made using FEMM 4.2 (*Finite Elements Method Magnetics*) computer program. A similar figure could be made to represent the $\Psi_{BC}(i_A, i_B)$ function, but the purpose here is to present the general properties of the current-flux characteristic in a simplified way, as it is impossible to present them for the whole $h^{-1}: \boldsymbol{\Psi} \to \boldsymbol{i}$ function.

It can be seen that the $\Psi_{AC}(i_A, i_B)$ function is very nonlinear only in relatively small regions of its domain, whereas in other regions it is close to a linear function. The function is close to linear near the point (0,0) (due to the linearity of the magnetizing curve for small magnetic field intensity) and in the regions where $|i_A| \gg 0$ and $|i_B| \gg 0$ and i_A, i_B have the same sign (due to the magnetic saturation). It is worth noting that these observation applies for the $\Psi_{BC}(i_A, i_B)$ function, but the position of the linear and nonlinear regions for the $\Psi_{AC}(i_A, i_B)$ and $\Psi_{BC}(i_A, i_B)$ are generally not the same in the space of currents. The main conclusion here is that the point sets of currents and fluxes, on which the approximation is based, should be very dense only in these nonlinear regions.
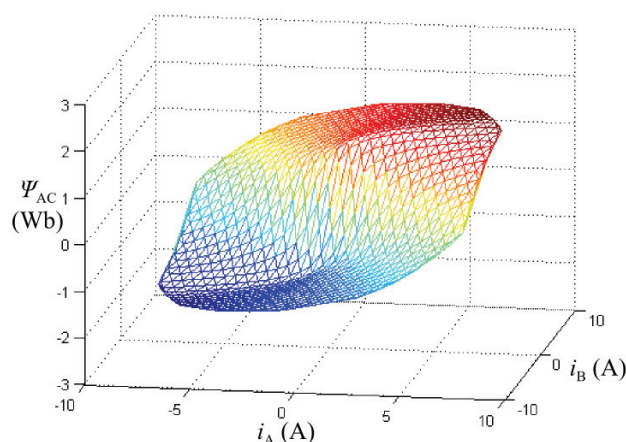

Fig. 2. A surface representation of the $\Psi_{AC} = g(i_A, i_B)$ function

The algorithm used to construct such sets is a simple iterative algorithm, based on the progressive insertion of new vertices into the vertices (points) sets of the currents and fluxes. A new vertex insertion means a determination of current values i_A^n, i_B^n, followed by the computation of corresponding fluxes $[\Psi_{AC}^n; \Psi_{BC}^n] = h^{-1}(i_A^n, i_B^n)|_{\varphi = \text{const}}$ using the FEM model of an electrical machine. After that, points $(i_A^n; i_B^n)$ and $(\Psi_{AC}^n; \Psi_{BC}^n)$ are put into respective sets of vertices.

Hence the algorithm for construction of the sets of currents and fluxes is as follows:
Triangulation of the actual sets of vertices (triangulation is the same in both currents and fluxes space),

 1) Computation of the approximation error (described in 4) in each simplex of the triangulation,
 2) *If* an error is larger than the assumed threshold ε *and* the size (in 2D: the surface) of the simplex is greater than the assumed one, insertion of a new vertex in the middle of the simplex.
 3) *If* there were vertices added into constructed sets in actual iteration *then* return to the beginning (continue the algorithm); *else* end the procedure.

In the beginning of the algorithm the number of elements in both sets is arbitrarily small. Such an approach ensures that the number of elements in the constructed sets is as small as possible, but the approximation is still performed with an error less than a given error ε. Another approach would be to simplify a big sets of vertices by getting rid of the redundant vertices. Such an approach can be found in literature [5], but it's hard to practically implement it in the considered case, because it would strongly lengthen the process of constructing the simplicial approximations by measurements or computation.

The described algorithm leads to good results irrespective of the initial points sets, i.e. after the application of the algorithm, the constructed sets are always more dense in expected, nonlinear regions of the spaces of the currents and fluxes. The number of iterations required to finish the algorithm is also satisfactory (for a construction of sets for the approximation of current-flux characteristic for an exemplary SynRM machine, the number of iterations was 7, with 21 points and 28 simplexes initially and 81 points and 148 simplexes after computation). The main disadvantage of the presented algorithm is the lack of a straightforward method of getting rid of redundant vertices, which can probably arise after every iteration. The aforementioned methods found in literature could also not be applied, as they require sets which are much denser than those appearing in the described algorithm.

4. Simplicial approximation error

In a Hamiltonian model it is assumed that energy losses (magnetizing and eddy current losses) are negligible. The magnetic field coenergy E_{cm} is therefore a state function and hence its change ΔE_{cm} along a closed path in state space is equal to 0. Using a simplicial approximation, this computation can only be linearly approximated. Along the edges of a given simplex S, vertices of which are $\boldsymbol{i}^K$, $\boldsymbol{i}^L$, $\boldsymbol{i}^M$ in currents space and $\boldsymbol{\Psi}^K$, $\boldsymbol{\Psi}^L$, $\boldsymbol{\Psi}^M$ in fluxes space, this approximation is given by a formula (2).

$$\Delta E_{\mathrm{cm}} = \frac{1}{2} \sum_{\substack{k=\mathrm{L,M,K} \\ j=\mathrm{K,L,M}}} \left(\Psi^k + \Psi^j \right) \left(\boldsymbol{i}^k - \boldsymbol{i}^j \right). \tag{2}$$

The mechanism of the ΔE_{cm} computation, but only for one component of the vector of fluxes, namely for a Ψ_{AC} component, is shown schematically in Figure 3. As a formula (2) involves scalar product, analogous figure could be made for a Ψ_{BC} component.
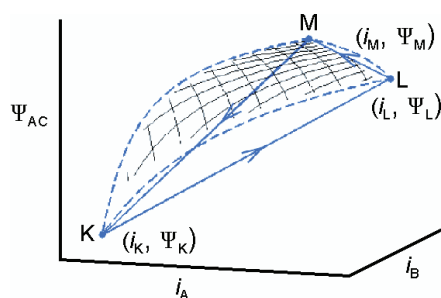

Fig. 3. A scheme of the mechanism of an error computation for one component,
namely Ψ_{AC}, of a flux vector

It can be noticed, that the absolute value of ΔE_{cm} would be higher the more curved the approximated function is in a given simplex S. The ΔE_{cm} can hence be used as a measure of an approximation error. Due to the practical reasons and the algorithm described in 3, it is better to use a relative error δE_{cm} equal to ΔE_{cm} divided by the average coenergy $\overline{E}_{\mathrm{cm}}$ computed in S, which is given by the formula (3):

$$\Delta \overline{E}_{\mathrm{cm}} = \frac{1}{3} \left(E_{\mathrm{cm}}^{\mathbf{K}} + E_{\mathrm{cm}}^{\mathbf{M}} + E_{\mathrm{cm}}^{\mathbf{L}} \right), \tag{3}$$

where $E_{\mathrm{cm}}^{\mathbf{K}}, E_{\mathrm{cm}}^{\mathbf{M}}, E_{\mathrm{cm}}^{\mathbf{L}}$ are the magnetic coenergy values in the vertices of the simplex S.
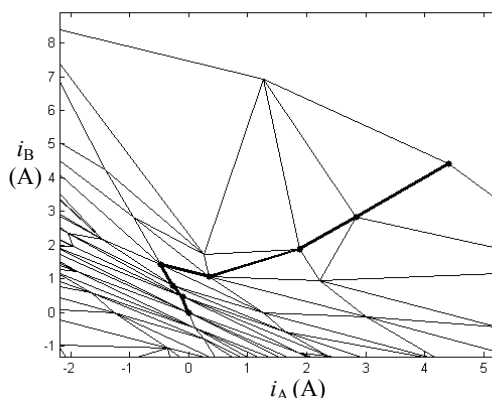

Fig. 4. The polygonal chain used for magnetic coenergy computation in the point (4.4 A; 4.4 A)

The value of the magnetic field coenergy $E_{cm}^{\mathbf{P}}$ in a given point $\mathbf{P}$, which belongs to the triangulated set of currents is obtained by the two-step procedure. First, a polygonal chain that begins in the point (0,0) and ends in the point P is found – segments of this polygonal chain are the edges of the triangulation and total length of this chain is the smallest possible number. Such a polygonal chain, found for a point (4,4 A; 4,4 A) is shown in Figure. 4.

Next, assuming that the chain is specified by $p + 1$ points, with P being the $(p + 1)$-th one, point (0,0) the 1st one and in the n-th point the values of current and flux are specified by $\boldsymbol{i}^n$ and $\boldsymbol{\Psi}^n$ respectively, $E_{cm}^{\mathbf{P}}$ can be computed using the formula (4):

$$E_{cm}^{\mathbf{P}} = \frac{1}{2} \sum_{n=1}^{p} \left(\Psi^{n+1} + \Psi^n \right) \left(\boldsymbol{i}^{n+1} - \boldsymbol{i}^n \right). \tag{4}$$

In the literature, an error which arises due to energy losses omission is stated as low, but nevertheless still discernible, for both the linear [8] and the rotating SRM machine (which is similar to the modelled SynRM machine) [6]. That way the approximation accuracy can be controlled to not be unnecessarily greater than the error already made because of the taken assumption. The exact value of the relative error δE_{cm} that is caused by the omitted effects was not found in the literature.

5. Triangulations of sets of vertices

A quality of the simplicial approximation relies strongly on a triangulation of constructed sets. The Delaunay triangulation algorithm, which is the most popular procedure used in practice, could not be performed on one set and used directly on the second set, as it could lead to ambiguities (some points can belong to two different simplexes, Figure 5., left) and as a result break some topological features of the approximated function.
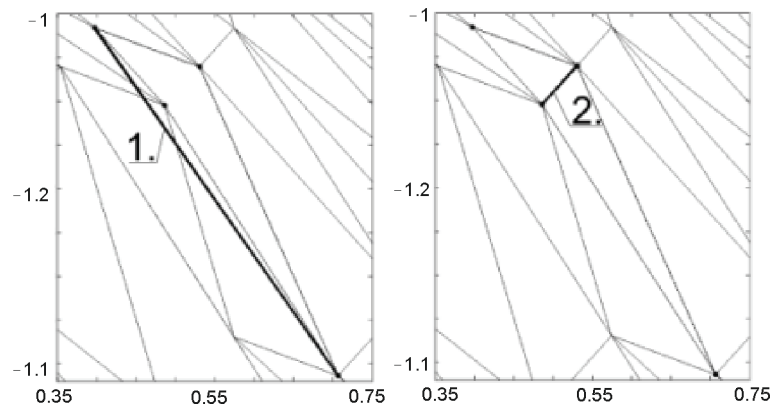

Fig. 5. Triangulation refinement by edge flipping

The ambiguities occur particularly when one of the triangulation's edges crosses a curved, nonlinear area. Such a situation is shown for an exemplary function in the Figure 6, with the edge P_1P_2 being the aforementioned edge. This breaks the monotonicity of the approximated function along the $P_{a'}$-$P_{b'}$-$P_{c'}$ line, which is a cause of the ambiguities. P_c is not a vertex in this triangulation. It can be noticed, that making an edge between points P_a and P_b and at the same time getting rid of the P_1P_2 edge would fix the issue.
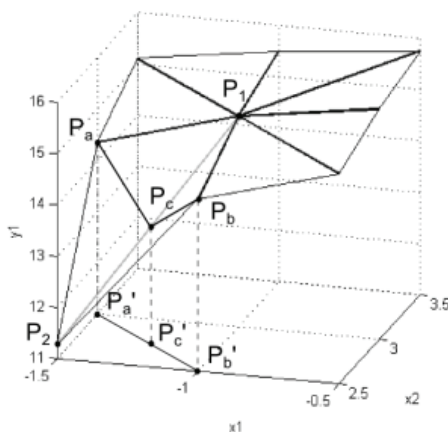

Fig. 6. Violation of monotonicity

A pair of simplexes forming a quadrilateral with ambiguities can be eliminated by flipping an edge, which is common to each simplex of this pair. Flipping an edge is a well-known practice for transitioning between various triangulations of the same set [3, 7]. A quadrilateral for which flipping an edge eliminates ambiguities is shown in Figure 5. On the left, edge 1 is shown as the cause of the simplex overlapping – edge 1 crosses other edges without any vertices (points) at the crossing places. Therefore edge 1 has to be flipped to get a locally good, unambiguous triangulation. A flipped edge 2, shown on the right, joints vertices which are the members of the simplexes previously adjacent to the edge 1, but which were not connected by an edge. As can be noticed, flipping an edge eliminates ambiguities.

As mentioned earlier, a valid data sets triangulation is required to properly approximate the $i = h(\mathbf{\Psi})$ function. To obtain such a triangulation, the following algorithm is used:
 1) Triangulation of set of fluxes using the Delaunay algorithm,
 2) Transfer of the obtained triangulation directly on the set of currents, i.e.:
    If $\mathbf{\Psi}^K\mathbf{\Psi}^L\mathbf{\Psi}^M$ form a simplex in fluxes space and $\boldsymbol{i}^K = h(\mathbf{\Psi}^K) \wedge \boldsymbol{i}^L = h(\mathbf{\Psi}^L) \wedge \boldsymbol{i}^M = h(\mathbf{\Psi}^M)$ then $\boldsymbol{i}^K\boldsymbol{i}^L\boldsymbol{i}^M$ form a simplex in space of current,
 3) Finding ambiguities and edges to be flipped in triangulated currents set,
 4) Triangulation of the set of fluxes using the Delaunay algorithm, with found edges as constraints,
 5) Transfer of the triangulation obtained in point 4) on the set of currents.

The triangulation of the set of fluxes, obtained in such a way, can be considered as a modification of the Delaunay triangulation (it is non-Delaunay only locally), whereas a triangula-

tion of the set of currents is generally non-Delaunay. The algorithm for finding a valid triangulation is based on the Delaunay triangulation of the set of fluxes, because fluxes are state variables in the considered, Hamiltonian model of an electromechanical system.

Getting an unambiguous triangulation can be a starting point for further improving a triangulation, e.g. using the criteria described in [4].

6. Features of the constructed approximation

In order to analyze the proposed algorithm for simplicial approximation construction, this method is used to approximate the current-flux characteristic of a prototype SynRM machine. During the computations the rotor of the machine was neither aligned nor unaligned, but it does not affect the generality of the proposed method, as it allows for the set construction regardless of the rotor angular position. The values of fluxes, required to construct a set of points in the space of fluxes, were computed using a FEM model of this machine. The relative error value that caused the insertion of a new vertex into a simplex was set to $\varepsilon = 5\%$ and the minimal simplex size was set to 0.3 space unit squared.

The set in the space of currents, which is the result of the proposed algorithm, is irregular (i.e. points in this set are not uniformly distributed across an interesting area) and thus its triangulation is further called a triangulation on an irregular set. The obtained triangulation is compared with a simplicial approximation based on the following sets: regular set of points in the space of currents and the set of corresponding points in the space of fluxes – triangulation of these sets is further called a triangulation on regular sets. The approximation based on such sets is taken into comparison because it is an effect of the most straightforward approach, where the currents values for the fluxes computation are chosen without any criteria and uniformly cover an interesting area in the space of currents. The number of points in both regular and irregular sets is the same.

The triangulated sets, both regular and irregular, are shown in Figure 6, and some features of both triangulations are shown in Table 1. Simplexes, the size (surface) of which was smaller than assumed (see algorithm in 3), were not taken into account.

Table 1. Features of constructed points sets

Set of vertices in **RI**	Approximation	
	Irregular	Regular
Number of vertices	81	81
Number of simplexes	148	148
Maximum $|\delta E_{cm}|$	0.043	0.483
Number of simplexes with $|\delta E_{cm}| > 0.05$	0	16

As shown in Figure 7, application of the proposed algorithm causes the set in the space of current to be more dense near the point (0; 0) and along a major axis of an elliptical area chosen as an interesting area, whereas in the space of fluxes, after using the algorithm, the set

is more uniform than the regular one. It can also be seen, that the Delaunay-like triangulation of the set of fluxes leads to long, thin simplexes in the space of currents, especially for simplexes lying along and near the major axis of the aforementioned ellipse.

a) irregular points set in **RΨ**

b) regular points set in **RΨ**

c) irregular points set in **RI**

d) regular points set in **RI**

e) approximation error computed for the approximation based on irregular sets

f) approximation error computed for the approximation based on regular sets
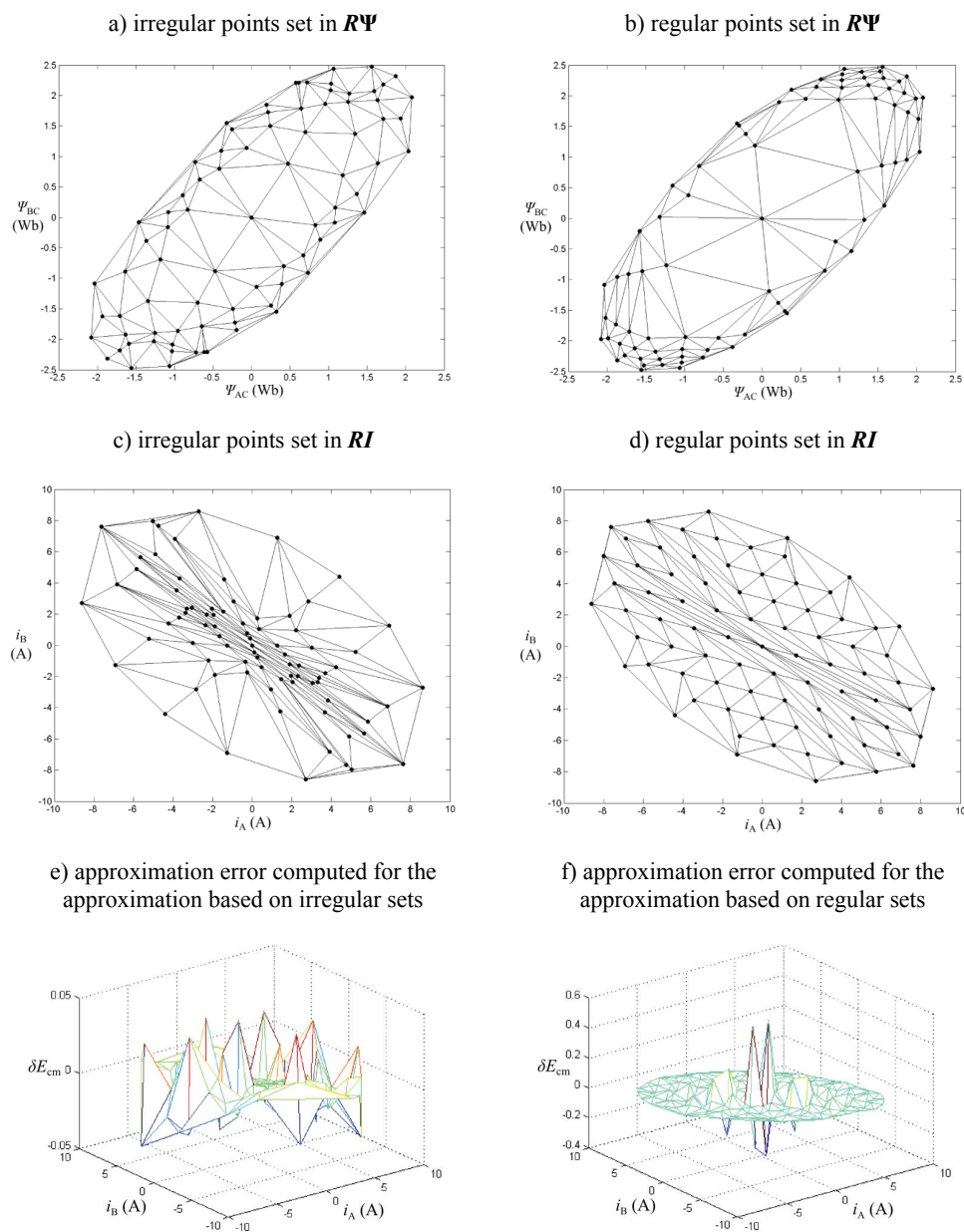

Fig. 7. Triangulated points sets in the spaces of currents and fluxes (a, b, c, d) and approximation errors (e, f) for both regular and irregular sets

In Figures 7e) and 7f) the surface representation of an approximation error is shown. As expected, an error computed for the approximation based on irregular sets is less than 5%, but is generally not much smaller than this value. An error computed for the approximation based on the regular sets is very large (nearly 50%) near the point (0; 0) in the space of currents, but decreases fast and is close to 0 for currents close to the boundary of the considered area. Regular sets are therefore too dense in this area.

To make a further comparison, solutions of Equation (1) were computed numerically. Solutions were computed for the approximation of the $i = h(\mathbf{\Psi})$ function based on both regular and irregular sets. The obtained solutions are compared with the solution obtained for the approximation based on very dense sets – 877 points and 1718 simplexes in triangulation – which is treated as a reference solution. The set of currents in the approximation used to obtain this reference solution is regular and is further called a dense regular set. Another approach would be to add additional points into the irregular sets. The sets constructed in such a way share points with irregular sets and could be hence compared with them more thoroughly. In the paper, additional points were added into the triangulated, irregular set of currents in centres of the mass of every simplex and in the centres of every edge, with corresponding points added into the set of fluxes. The sets constructed in such a way are further called dense irregular sets. It is worth noting that dense irregular sets are similar to the sets, that would have been results of the proposed algorithm, if the relative error value ε was set to be less than 1% (although points in the centres of the edges would not be added). Dense irregular sets have 445 points and 862 simplexes in triangulation

The equation (1) was solved for:

$$e_A = 100\sqrt{2}\,\sin(2\pi ft)\,\text{V},$$

$$e_B = 100\sqrt{2}\,\sin\!\left(2\pi ft + \frac{2\pi}{3}\right)\text{V},$$

$$e_C = 100\sqrt{2}\,\sin\!\left(2\pi ft - \frac{2\pi}{3}\right)\text{V},$$

$r_A = r_B = r_C = 13\ \Omega$; $f = 50\ \text{Hz}$ – voltage frequency; $\varphi = \text{const.}$

In Figure 8 the time plots of the i_A current and the Ψ_{AC} flux are shown. Figures show one period of the obtained time plots, taken in steady state. Analysis of these results is sufficient to state the general properties of the solutions computed for various the approximations, as time plots of the i_B current and the Ψ_{BC} resemble time plots of the i_A current and the Ψ_{AC} flux, respectively.

It can be noticed that solutions for flux are not affected by the type of set and both are close to both reference solutions. Large differences can be noticed though for time plots of i_A: the solution for the irregular set is much closer to the reference solution than the solution for the regular set. The largest differences are located in the neighbourhood of the local extrema of the current time plots. In this region, in the solution for the regular sets sudden changes in the i_A value can be noticed. This is caused by sudden changes in the values of derivatives

$$\frac{\partial i_A}{\partial \Psi_{AC}}, \quad \frac{\partial i_B}{\partial \Psi_{AC}}, \quad \frac{\partial i_A}{\partial \Psi_{BC}}, \quad \text{and} \quad \frac{\partial i_B}{\partial \Psi_{BC}},$$

as a phase space trajectory crosses an edge between two simplexes (Fig. 9). In case of the irregular sets, changes in values of derivatives are much slower (Fig. 8), which results in a much smoother approximation.

a) Time plots of the i_A current for different approximations

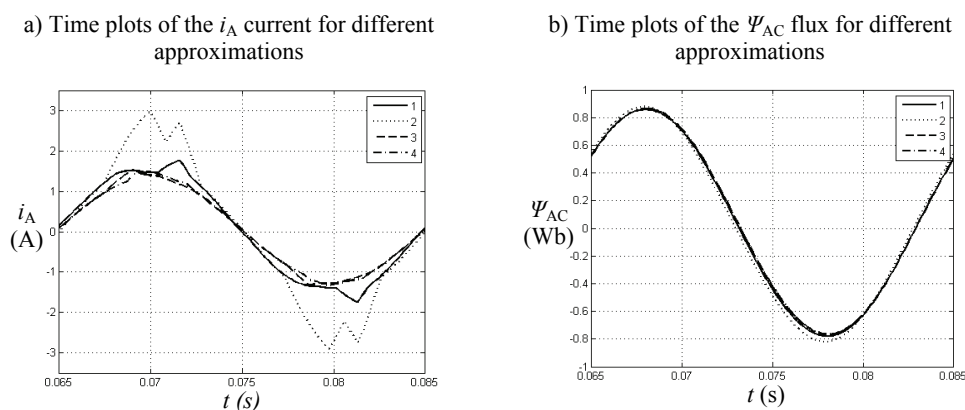b) Time plots of the Ψ_{AC} flux for different approximations

Fig. 8. Time plots of current and flux as a solutions of Eq. (1). Solutions obtained for approximations based on: 1 – irregular sets, 2 – regular sets, 3 – dense regular sets and 4 – dense irregular sets
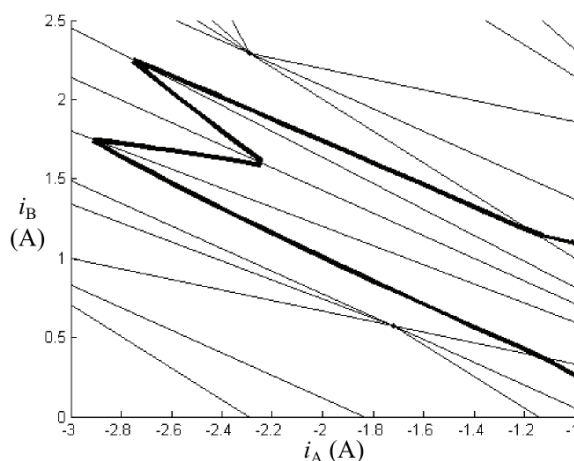

Fig. 9. A phase space trajectory in the space of currents, obtained for regular sets (bold line), against the triangulation of the regular set of currents

Parts of the computed trajectory in the space of currents were located in the areas, where the current-flux characteristic is nonlinear, although the trajectory does not pass through the regions of high magnetic saturation. In order to explore the behaviour of the approximation based on various sets, when trajectory in the space of currents passes from one region where

current-flux characteristic is linear due to the saturation, to the region, where it is linear due to small values of magnetic field intensity, another computation were made. In this computation the equation (1) was solved for:

- $e_A = e_B = e_C = 0$,
- initial current values set to $i_A(t = 0) = 4$ A, $i_B(t = 0) = 4$ A, so that the point corresponding to these values lies far in the region of saturation in the space of currents.

Obtained results were computed for the approximation based on various sets of currents and fluxes. A part of time plots of i_A current, corresponding to the part of trajectory in the space of currents that passes through the region of highly nonlinear current-flux characteristic, is presented in the Figure 10. Time plots obtained for the approximation based on both dense regular and dense irregular sets are similar. The time plot obtained for the approximation based on irregular sets is consistent with these reference solutions, although differences are clearly visible (e.g. for the time t = 0.005 s). As expected, the time plot obtained for regular sets differ the most form the aforementioned three. In this time plots a non-differentiable points are also the most visible, which confirms observation and conclusions made earlier in this paragraph.
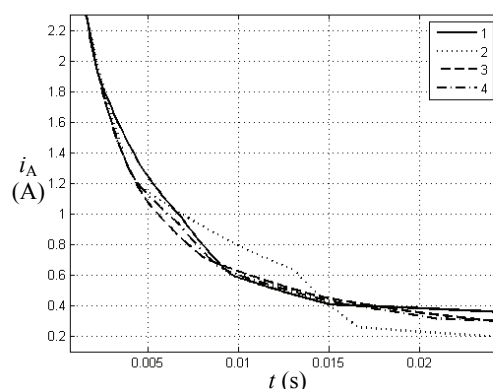

Fig. 10. A time plots of current in a computation with phase voltages set to 0 and non-zero initial current values, obtained for approximations based on: 1 – irregular sets, 2 – regular sets, 3 – dense regular sets and 4 – dense irregular sets

7. Conclusions

A construction of a simplicial approximation on an irregular set of vertices decreases the maximum approximation error and a number of simplexes with an error higher than 5% (which was an acceptable error) compared with the simplicial approximation on a regular set. The approximation based on irregular sets is more suited for a mathematical model of an electrical machine, as it approximates a current-flux characteristic more precisely and smoothly than the approximation based on regular sets, especially in nonlinear areas of the approximated characteristic.

During the construction of the simplicial approximation on an irregular set and without the ability to control of the way this set is triangulated, ambiguities can occur. The way to eliminate them is to find ambiguous simplexes and flip one of the edges of a quadrilateral to which they belong.

The proposed method of constructions of the sets of currents and fluxes applies only for the FEM computation of the machine with a locked rotor. To include a rotor's motion into the model, a separate approximation should be constructed for every angular position in an assumed set, e.g. for angular positions from 0° to 90°, every 1°. This approach requires large amount of data – another approach would be to use the modified Park transform and construct the model in *dq* reference frame. Comparison of these two approaches should be the aim of further research.

References

[1] Agoston M.K., *Computer Graphics and Geometric Modeling – Mathematics*. Springer (2005).
[2] Burlikowski W., *Hamiltonian model of electromechanical actuator in natural reference frame, Part 1&2*. Archives of Electrical Engineering 60(3): 317-348 (2011).
[3] De Loera J.A., Rambau J., Santos F., *Triangulations. Structures for Algorithms and Applications.* Springer (2010).
[4] Dyn N., Levin D., Rippa S., *Data dependent triangulations for piecewise linear interpolation.* IMA Journal of Numerical Analysis 10: 137-154 (1990).
[5] Groff R.E., *Piecewise Linear Homeomorphism for Approximation of Invertible Maps.* PhD Thesis, The University of Michigan (2003).
[6] Marčič T., Stumberger G., Stumberger B., *Analyzing the Magnetic Flux Linkage Characteristics of Alternating Current Rotating Machines by Experimental Method.* IEEE Transactions on Magnetics 47(9): 2283-2291 (2011).
[7] Scheuermann G., Hagen H, *A Data Dependent Triangulation for Vector Fields.* Computer Graphics International, pp. 96-102 (1998).
[8] Stumberger G., Stumberger B., Dolinar D., Tezak O., Hameyer K., *Nonlinear model of linear synchronous reluctance motor for real time applications.* COMPEL 23(1): 316-327 (2002).